Inorg. Chem. **2008**, *47*, 7360−7365

Binding Properties of Solvatochromic Indicators [Cu(X)(acac)(tmen)] (X = PF_6^- and BF_4^-, $acac^-$ = Acetylacetonate, tmen = *N,N,N′,N′*-Tetramethylethylenediamine) in Solution and the Solid State

Shin-ichiro Noro,*,† Nobuhiro Yanai,‡ Susumu Kitagawa,|| Tomoyuki Akutagawa,†,§ and Takayoshi Nakamura*,†,§

Research Institute for Electronic Science, Hokkaido University, Sapporo 060-0812, Japan, Department of Synthetic Chemistry and Biological Chemistry, Graduate School of Engineering, Kyoto University, Kyoto 615-8510, Japan, Institute for Integrated Cell-Material Sciences (iCeMS), Kyoto University, Kyoto 606-8501, Japan, and CREST, Japan Science and Technology Agency (JST), Kawaguchi 332-0012, Japan

Received April 17, 2008

The solvatochromic indicator [Cu(acac)(tmen)(H_2O)]·PF_6 (**1**·H_2O) has been synthesized and crystallographically characterized. **1**·H_2O binds an H_2O molecule at the Cu(II) axial site, while the PF_6^- anion is coordination free. The binding properties of [Cu(PF_6)(acac)(tmen)] (**1**) and [Cu(BF_4)(acac)(tmen)] (**2**) have been investigated in solution and the solid state. The donor number of the PF_6^- anion (DN_{PF6}) was determined from the UV−vis spectra of **1** in 1,2-dichloroethane. The value of DN_{PF6} of the PF_6^- anion is slightly larger than that of the tetraphenylborate anion (BPh_4^-), which is known as a noncoordinating anion. In the solid state, **1** and **2** reversibly bind and release H_2O molecules at the Cu(II) axial sites. The coordinated H_2O molecules in **2** are more easily removed than those in **1** because of the strong Lewis basicity of the BF_4^- anion compared to the PF_6^- ion. The lower melting point of **1** versus **2** is attributed to the loose binding of the PF_6^- anions to the Cu(II) centers, which induces the dynamic nature of the crystal.

Introduction

Solvatochromism can be broadly defined as the influence of the "medium" on the electronic absorption and emission spectra of molecules. The word "medium" should be taken in a very wide sense since it may include solids, micelles, organized molecular films, and even a vacuum, apart from liquid solvents. The solvatochromic shifts are only one aspect of the influence of the medium on the energy states of molecules and are important not only for the description of the relative energies of electronic states of molecules but also for the experimental determination of some important physical properties such as the dipole moment, the polarizability, and the higher multipole moments of molecules.[1] Having such characteristics, a large number of solvatochromic molecules have been used as probes for a detection of proteins, nucleic acids, enzymes, ions of biological significance (Ca(II), K(I), and various heavy metal cations), and also materials on a macroscopic scale (e.g., cell membranes).[1b] In addition, the solvatochromic shifts often provide information about specific interactions such as hydrogen bonding.

It is known that the mixed-ligand Cu(II) complex [CuX(acac)(tmen)] ($acac^-$ = acetylacetonate, tmen = *N,N,N′,N′*-tetramethylethylenediamine, and X = anion) and its derivatives with β-diketonate and diamine ligands show a pronounced solvatochromism.[2] [CuX(acac)(tmen)] is soluble in various organic solvents, which is a necessary condition to observe pronounced solvatochromism. Furthermore, the strong Jahn−Teller effect on the Cu(II) ions leads to a continuous color change with variation of the Lewis acid and Lewis base interaction between the Cu(II) complex and the respective ligand. Therefore, [CuX(acac)(tmen)] has been used as a solvatochromic Lewis acid and Lewis base indicator. A large number of donor numbers of solvents (DN) and also anions (DN_X, X = anion) have been determined using these solvatochromic indicators. However, the value of the DN_{PF6} of the PF_6^- anion has not yet been determined.

* To whom correspondence should be addressed. E-mail: noro@es.hokudai.ac.jp (S.-i.N.), tnaka@es.hokudai.ac.jp (T.N.).
† Hokkaido University.
‡ Department of Synthetic Chemistry and Biological Chemistry, Graduate School of Engineering, Kyoto University.
|| Institute for Integrated Cell-Material Sciences (iCeMS), Kyoto University.
§ CREST, JST.

10.1021/ic800685z CCC: $40.75
Published on Web 07/25/2008

The PF_6^- anion is a very weak Lewis base and hardly coordinates to metal ions. Therefore, it has been used as an inert counteranion for a large number of cationic metal complexes. We have reported on metal complexes with weakly metal-coordinated PF_6^- anions (Cu−F distance = 2.583(3) and 2.676(4) Å).[3] These Cu(II) complexes are obtained in the presence of H_2O, which is a strong Lewis base. Nevertheless, it is surprising that the weak Lewis base PF_6^- anions coordinate to the axial sites of the Cu(II) ions instead of H_2O. The reason why the PF_6^- anion can coordinate is thought to be as follows. The axial bond distance between a Lewis acid Cu(II) ion and a Lewis base molecule is longer than the general coordination bond length because of the Jahn−Teller effect, resulting in a very weak acid−base interaction. Because the PF_6^- molecule has a negative charge, an electrostatic interaction exists between a cationic Cu(II) ion and an anionic PF_6^- molecule. In Cu(II) complexes, the acid−base interaction probably contributes to the axial bond in competition with electrostatic interaction because the electrostatic interaction is generated over a long distance that is proportional to r^{-1} (r = intermolecular distance). Therefore, Cu(II) complexes form with weakly coordinated PF_6^- anions by controlling the reaction conditions. Recently, we have succeeded in synthesizing an infinite Cu(II) complex that shows an interesting dynamic property of PF_6^- anions.[4] $\{[Cu(bpetha)_2(acetone)_2]\cdot 2PF_6\}_n$ (bpetha = 1,2-bis(4-pyridyl)ethane) constructed from one-dimensional double chains shows reversible acetone adsorption and desorption properties. In the presence of acetone guest molecules, the PF_6^- anions are coordination free, while the PF_6^- anions approach the vacant Cu(II) axial sites after the removal of acetone molecules. This dynamic nature of the PF_6^- anions is derived from the competition between the acid−base and electrostatic interactions in the formation of the Cu(II) axial bonds.

From such a background, it is expected that a quantitative evaluation of the DN_{PF6} of the PF_6^- anion is important for selecting counteranions to create the desired coordination complexes. In this manuscript, we report on (i) the synthesis and crystal structure of the mononuclear Cu(II) complex formulated as $[Cu(acac)(tmen)(H_2O)]\cdot PF_6$ (**1**·H_2O), (ii) the Lewis basicity (DN_{PF6}) of the PF_6^- anion, which was evaluated using the desolvated complex **1** as a solvatochromic indicator, and (iii) the binding properties of **1** and $[Cu(BF_4)(acac)(tmen)]$ (**2**)[2c] in the solid state, because the binding properties of the solvatochromic indicators [CuX(acac)(tmen)] in solid state have been little studied.

Experimental Section

The chemicals used were as obtained, without any further purification. Elemental analysis (C, H, and N) was performed using a PerkinElmer Model 240C elemental analyzer. Infrared (IR) spectra measurements were carried out using a KBr disk on a PerkinElmer Spectrum 2000 spectrophotometer with a resolution of 4 nm. UV−vis spectra in H_2O, 1,2-dichloroethane (DCE), acetonitrile (MeCN), and dimethylformamide (DMF) were measured using a PerkinElmer Lambda-19 spectrophotometer with a resolution of 1 nm. UV−vis reflection spectra were recorded using a Hitachi U-3500 spectrophotometer with a resolution of 1 nm. X-ray diffraction (XRD) data were collected using a Rigaku RINT-Ultima III diffractometer employing Cu Kα radiation. Thermogravimetric analysis (TGA) and differential thermal analysis (DTA) were performed using a Rigaku Thermo Plus 2/TG-DTA8120 over the temperature range 298−773 K under a N_2 atmosphere. NMR experiments were carried out on a JEOL JNM-LA300WB spectrometer operating at a resonance frequency of 121.5 MHz for ^{31}P at room temperature. A 7 mm double-resonance magic-angle spinning (MAS) probe was used at a spinning speed in the range 4.0−4.3 kHz. The spectra were obtained using a single-pulse 90° irradiation (pulse length = 5.7 μs) with proton decoupling. $NH_4H_2PO_4$ (δ = 1.00 ppm) was used as a reference sample.

Preparation of [Cu(PF$_6$)(acac)(tmen)] (1). KPF_6 (1.84 g, 10 mmol) was added to 20 mL of an EtOH solution containing $Cu(ClO_4)_2\cdot 6H_2O$ (0.926 g, 2.5 mmol). The obtained suspension was stirred for 30 min, and then filtered. To the sky blue filtrate, 20 mL of H_2O and then the solution (10 mL H_2O and 10 mL EtOH) containing acetylacetone (0.257 mL, 2.5 mmol) and *N,N,N′,N′*-tetramethylethylenediamine (0.377 mL, 2.5 mmol) was added. Na_2CO_3 (0.132 g, 1.25 mmol) was added to neutralize the obtained dark blue suspension. The suspension was stirred overnight and then filtered. The filtrate was allowed to stand for a period of one week to yield a dark blue crystalline sample with the formula $[Cu(acac)(tmen)(H_2O)]\cdot PF_6$ (**1**·H_2O). After filtration, the crystals were washed with H_2O and dried at room temperature in vacuo. Anal. Calc. for $C_{11}H_{23}Cu_1F_6N_2O_2P_1$, C = 31.17; H = 5.47; N = 6.61. Found, C = 31.10; H = 5.41; N = 6.68. IR (KBr pellet, cm^{-1}): 3020 w, 2995 w, 2929 w, 2909 m, 2888 w, 2859 w, 2811 w, 1582 s, 1526 s, 1476 m, 1424 m, 1375 s, 1284 m, 1247 w, 1200 w, 1127 w, 1050 w, 1023 m, 1002 w, 953 m, 935 w, 839 s, 810 m, 767 w, 739 w, 686 w, 656 w, 600 w, 557 s, 458 w, and 424 w.

Preparation of [Cu(BF$_4$)(acac)(tmen)] (2). $AgBF_4$ (62.0 mg, 3.18×10^{-1} mmol) was added to 10 mL of an EtOH solution of [CuCl(acac)(tmen)] (100 mg, 3.18×10^{-1} mmol).[2g,5] The obtained suspension was stirred for a period of 30 min and then filtered. The filtrate was concentrated using a rotary evaporator, and excess hexane was added to the filtrate. Purple microcrystals were obtained after a period of 2 h. These were washed with hexane and dried at room temperature in vacuo. Anal. Calcd for $C_{11}H_{23}B_1Cu_1F_4N_2O_2$, C = 36.13; H = 6.34; N = 7.66; Cl = 0.00. Found, C = 35.96; H = 6.19; N = 7.60; Cl = 0.0. IR (KBr pellet, cm^{-1}): 3009 w, 2981 w, 2964 w, 2896 m, 2856 w, 2799 w, 1591 s, 1525 s, 1470 m, 1434 m, 1386 s, 1277 m, 1249 w, 1204 w, 1126 m, 1098 s, 1083 s, 1029 s, 953 m, 934 w, 809 m, 771 w, 680 w, 669 w, 656 w, 601 w, 534 w, 521 w, 482 w, 453 w, 437 w, and 419 w.

(1) (a) Reichardt, C. *Chem. Rev.* **1994**, *94*, 2391–2358. (b) Suppan, P.; Ghoneim, N. *Solvatochromism*; The Royal Society of Chemistry: Cambridge, 1997.

(2) (a) Fukuda, S.; Sone, K. *Bull. Chem. Soc. Jpn.* **1972**, *45*, 465–469. (b) Soukup, R. W.; Sone, K. *Bull. Chem. Soc. Jpn.* **1987**, *60*, 2286–2288. (c) Linert, W.; Jameson, R. F.; Taha, A. *J. Chem. Soc., Dalton Trans.* **1993**, 3181–3186. (d) Linert, W.; Fukuda, Y.; Camard, A. *Coord. Chem. Rev.* **2001**, *218*, 113–152. (e) Spange, S.; Reuter, A.; Linert, W. *Langmuir* **1998**, *14*, 3479–3483. (f) Linert, W.; Taha, A. *J. Coord. Chem.* **1993**, *29*, 265–276. (g) Fukuda, Y.; Kimura, H.; Sone, K. *Bull. Chem. Soc. Jpn.* **1982**, *55*, 3738–3741. (h) Fukuda, Y.; Sato, N.; Hoshino, N.; Sone, K. *Bull. Chem. Soc. Jpn.* **1981**, *54*, 428–432. (i) Camard, A.; Ihara, Y.; Murata, F.; Mereiter, K.; Fukuda, Y.; Linert, W. *Inorg. Chim. Acta* **2005**, *358*, 409–414. (j) Fukuda, Y.; Yasuhira, M.; Sone, K. *Bull. Chem. Soc. Jpn.* **1985**, *58*, 3518–3523.

(3) Noro, S.; Kitaura, R.; Kondo, M.; Kitagawa, S.; Ishii, T.; Matsuzaka, H.; Yamashita, M. *J. Am. Chem. Soc.* **2002**, *124*, 2568–2583.

(4) Noro, S.; Horike, S.; Tanaka, D.; Kitagawa, S.; Akutagawa, T.; Nakamura, T. *Inorg. Chem.* **2006**, *45*, 9290–9300.

(5) Jalilehvand, F.; Ishii, Y.; Hidai, M.; Fukuda, Y. *J. Chem. Soc., Dalton Trans.* **1996**, 3251–3256.

Table 1. Crystallographic Data for $1 \cdot H_2O$

formula	$C_{11}H_{25}CuF_6N_2O_3P$
fw	441.84
lattice	monoclinic
a, Å	9.0330(13)
b, Å	18.810(3)
c, Å	11.5638(13)
β, deg	108.306(3)
V, Å^3	1865.4(4)
space group	$P2_1/n$
Z	4
ρ (calc.) g cm^{-3}	1.573
F(000)	908.00
μ (Mo Kα), cm^{-1}	13.25
radiation (λ, Å)	0.71073
temp., K	173
R^a	0.0464
$R_w{}^b$	0.0671
GOF	1.064
no. of observations	3310
no. of variables	240

$^a R = \sum||F_o| - |F_c||/\sum|F_o|$. $^b R_w = [\sum w(|F_o| - |F_c|)^2/\sum wF_o^2]^{1/2}$.

X-ray Structural Analysis. X-ray diffraction measurements on $1 \cdot H_2O$ were performed using a Rigaku RAXIS-RAPID imaging plate diffractometer using graphite-monochromated Mo Kα radiation ($\lambda = 0.71073$ Å). The data were corrected for Lorentz and polarization effects. The structure was solved using direct methods (SIR2002)[6] and expanded using Fourier techniques.[7] All nonhydrogen atoms were refined anisotropically. All the hydrogen atoms were refined using the riding model. The refinements were carried out using full-matrix least-squares techniques on F^2. All calculations were performed using the CrystalStructure crystallographic software package.[8] The crystal data are summarized in Table 1. The crystallographic data in CIF format are available from the Cambridge Crystallographic Data Centre, CCDC reference number 648025.

Results and Discussion

Although a large number of mononuclear Cu(II) complexes [CuX(acac)(tmen)] (X = BPh_4^-, BF_4^-, ClO_4^-, CO_3^{2-}, $CF_3SO_3^-$, NO_3^-, CN^-, I^-, $MeCO_2^-$, SCN^-, Br^-, N_3^-, OH^-, Cl^-, and NCO^-) have been synthesized, crystallographic characterization has only been performed on the complex [CuCl(acac)(tmen)].[5] The complex $1 \cdot H_2O$ is the second example where the crystal structure has been determined. Figure 1 shows the coordination geometry around the Cu(II) center of $1 \cdot H_2O$. In $1 \cdot H_2O$, the Cu(II) ion has a square pyramidal environment with acac$^-$ and tmen ligands in the basal plane and H_2O molecules at the axial site (Cu−O(H_2O) = 2.377(2) Å). The axial bond distance of $1 \cdot H_2O$ is shorter than those of [Cu(trop)(tmen)(DCE)]$\cdot BPh_4$ (trop$^-$ = tropolonate, Cu−Cl = 3.580(1) Å) and [Cu(trop)(tmen)(acetone)]$\cdot BPh_4$ (Cu−O = 2.502(2) Å),[2i] which is reasonable, because the value of DN of H_2O (19.5) is higher than that of DCE (0) and acetone (17.0). The calculated value of the τ factor,

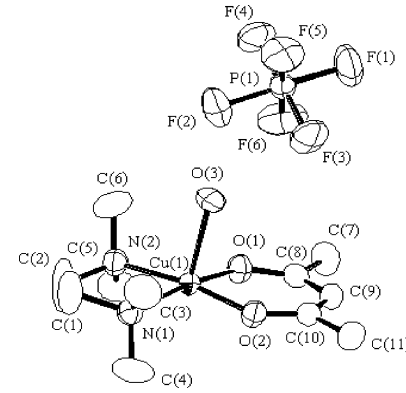

Figure 1. ORTEP (Oak Ridge Thermal Ellipsoid Plot) view of $1 \cdot H_2O$. The hydrogen atoms have been omitted for clarity.

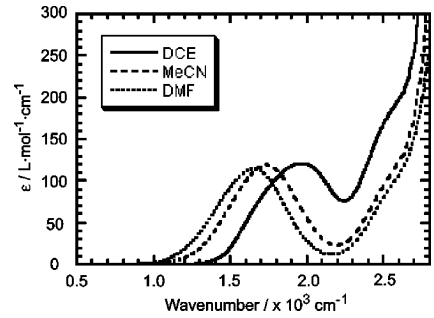

Figure 2. UV−vis spectra of **1** in DCE, MeCN, and DMF.

which is applicable to five-coordinate structures as an index of the degree of trigonality within the structural continuum between trigonal bipyramidal and square pyramidal,[9] was $\tau = 0.05$, indicating a strong square pyramidal character (the value of τ for a perfect square pyramidal and trigonal bipyramidal metal environment is $\tau = 0$ and $\tau = 1$, respectively). This value is slightly smaller than that of [CuCl(acac)(tmen)] ($\tau = 0.10$). None of the PF_6^- anions are related to either the coordination or the hydrogen bonds in the crystal. The H_2O molecules binding to the Cu(II) axial sites are easily removed from the crystal lattice at room temperature under vacuum, forming [Cu(PF_6)(acac)(tmen)] (**1**). The results of the elemental analysis and TGA (Supporting Information, Figure S1) support complete dehydration.

First, we checked the binding properties of **1** in solution. UV−vis spectra in solution were measured to evaluate the donor ability of the PF_6^- anions quantitatively. Figure 2 shows the UV−vis spectra of **1** in DCE, MeCN, and DMF. The color of a solution of **1** strongly depended on the type of solvent: the colors of the DCE, MeCN, and DMF solutions were purple, blue, and sky blue, respectively (see Supporting Information, Figure S2). As shown in Figure 2 and Supporting Information, Table 2, the absorption maxima of a d−d transition shifts to lower frequencies as the donor ability of the solvent increases,[10] indicating that PF_6^- anions hardly coordinate to the Cu(II) axial sites of **1** in MeCN and DMF. Because DCE has almost no coordination ability compared to MeCN and DMF, the PF_6^- anions can interact with the

(6) *SIR 2002* Burla, M. C.; Camalli, M.; Carrozzini, B.; Cascarano, G. L.; Giacovazzo, C.; Polidori, G.; Spagna, R. *J. Appl. Crystallogr.* **2003**, *36*, 1103.
(7) *DIRDIF-94* Beurskens, P. T.; Admiraal, G.; Beurskens, G.; Bosman, W. P.; de Gelder, R.; Israel, R.; Smits, J. M. M. *The DIRDIF-94 program system, Technical Report of the Crystallography Laboratory*; University of Nijmegen: The Netherlands, 1994.
(8) *Crystal Structure Analysis Package*, Crystal Structure 3.7.0; Rigaku and Rigaku/MSC: The Woodlands, TX, 2000−2005.
(9) Addison, A. W.; Rao, T. N.; Reedijk, J.; van Rijn, J.; Verschoor, G. C. *J. Chem. Soc., Dalton Trans.* **1984**, 1349–1356.
(10) Gutman, V. *The Donor−Acceptor Approach to Molecular Interactions*; Plenum Press: New York, 1978.

Table 2. Absorption Maxima (10^3 cm^{-1}) for [CuX(acac)(tmen)] (X = anion)

anion	solid	DCE	MeCN	DMF
BPh_4^-	20.0	20.0	17.5	16.6
PF_6^-	**20.0**	**19.6**	**17.3**	**16.5**
BF_4^-	18.9	19.0		
ClO_4^-	18.6	18.6	17.3	16.6
CO_3^{2-}	17.5	17.8		
$CF_3SO_3^-$	17.2	17.2		
NO_3^-	16.5	16.5		
CN^-		15.5		
I^-	15.2	15.2	17.1	16.3
$MeCO_2^-$		15.1		
SCN^-	14.8	14.7	15.7	16.2
Br^-	14.5	14.4	15.6	16.2
N_3^-	14.4	14.3	15.0	15.3
OH^-		14.2		
Cl^-	14.1	14.0	14.5	14.7
NCO^-	13.4	13.3	13.7	14.0

Table 3. Donor Numbers of Anions in DCE (DN_{anion}) and Apparent Donor Numbers of Anions Dissolved in Various Solvents ($DN_{anion,solv}$) for [CuX(acac)(tmen)] (X = Anion)

	DN_{anion}	apparent donor number ($DN_{anion,solv}$)	
	DCE	MeCN	DMF
BPh_4^-	0.00	−1.20	0.39
PF_6^-	**2.18**	**0.97**	**2.56**
BF_4^-	6.03	4.83	6.42
ClO_4^-	8.44	7.24	8.83
CO_3^{2-}	13.3	12.1	13.6
$CF_3SO_3^-$	16.9	15.7	17.3
NO_3^-	21.1	19.9	21.5
CN^-	27.1	25.9	27.5
I^-	28.9	27.7	29.3
$MeCO_2^-$	29.5	28.3	29.9
SCN^-	31.9	30.7	32.3
Br^-	33.7	32.5	34.1
N_3^-	34.3	33.1	34.7
OH^-	34.9	33.7	35.3
Cl^-	36.2	34.9	36.5
NCO^-	40.4	39.2	40.8
DN_{solv}	0.0	14.1	26.6
AN_{solv}	16.7	18.9	16.0

Cu(II) axial sites in a DCE solution. The donor number in DCE (DN_{PF6}) and apparent donor numbers in MeCN and DMF ($DN_{PF6,MeCN}$ and $DN_{PF6,DMF}$, respectively) of the PF_6^- anion can be expressed as

$$DN_{X,solv} = 129.6 - 0.548AN_{solv} - 0.00602\nu_{max}(DCE) \quad (1)$$

where AN_{solv} and ν_{max}(DCE) are the acceptor number of the solvent and the absorption maxima in a DCE solution, respectively.[2c] The values of DN_{PF6}, $DN_{PF6,MeCN}$, and $DN_{PF6,DMF}$ were 2.18, 0.97, and 2.56, respectively.[11] Table 3 lists the donor numbers of anions (DN_X and $DN_{X,solv}$) in DCE, MeCN, and DMF. The donor ability of the PF_6^- anion is slightly larger than that of the BPh_4^- anion, which is known as a noncoordinating anion. Therefore, these results clearly indicate that the Cu(II) complex **1** with the PF_6^- anion is a good solvatochromic indicator, as is [Cu(acac)(tmen)]·

(11) The donor numbers of anions (DN_X and $DN_{X,solv}$) are affected by the AN_{solv} of solvents. As shown in Table 3, the AN_{solv} of MeCN is larger than those of DCE and DMF, which causes a weakening of the donor ability of anions. Therefore, the $DN_{PF6,MeCN}$ becomes smaller than DN_{PF6} and $DN_{PF6,DMF}$.

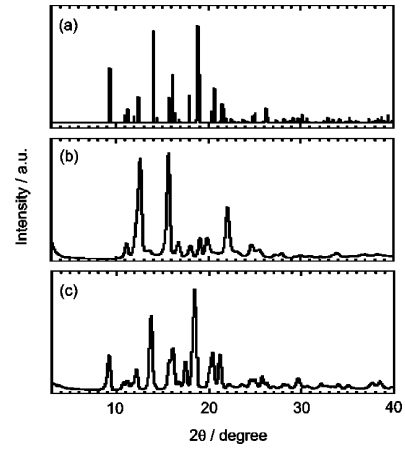

Figure 3. XRD patterns of (a) **1**·H_2O simulated from the X-ray single crystal structure, (b) **1**, and (c) **1**·H_2O at 298 K.

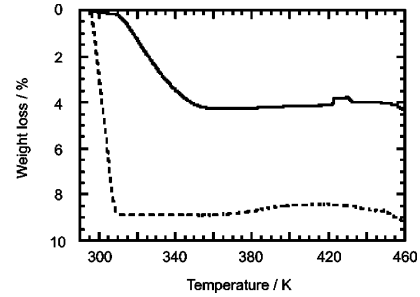

Figure 4. TGA curves of **1**·H_2O (solid line) and **2**·H_2O (dotted line).

BPh_4. Despite the very weak coordination ability of the PF_6^- anion, as well as the BPh_4^- anion, some Cu(II) coordination polymers with coordinated PF_6^- anions have been reported.[3] Therefore, the formation of Cu(II)−PF_6^- bonds is mainly attributed to the electrostatic interaction between the Cu(II) cation and the PF_6^- anion.

Next, we checked the binding properties of **1** in the solid state. The XRD pattern of the desolvated compound **1** (Figure 3b) is different from the calculated pattern of **1**·H_2O (Figure 3a), indicative of the formation of a new assembled structure on removal of the H_2O molecules. When the dehydrated compound **1** was exposed to H_2O vapor, then a rebinding of the H_2O molecules at the Cu(II) axial site was observed. The color of the sample changed from purple to blue. In the TGA profile of the exposed compound (Figure 4), the observed weight loss of about 4.3% up to 373 K corresponds to the removal of the H_2O molecules from the compound, which shows that the complex−H_2O ratio was 1:1. This ratio is consistent with the results of the single-crystal X-ray diffraction analysis. The XRD pattern of the exposed compound (Figure 3c) is markedly different from that of **1** and similar to the calculated pattern of **1**·H_2O. Therefore, the adsorption and desorption of H_2O in **1** is reversible. Figure 5 shows the solid-state ^{31}P NMR spectra of **1** and **1**·H_2O at 298 K. In general, the spectra of the PF_6^- anion have a septet pattern due to the spin−spin coupling of the ^{19}F nucleus ($I = 1/2$) with the ^{31}P nucleus. In **1**·H_2O, a septet pattern was observed, but the observed spectra of **1** is broader and its position (−153.1 ppm) was shifted upfield relative to that of **1**·H_2O (−136.7 ppm), which was attributed to the

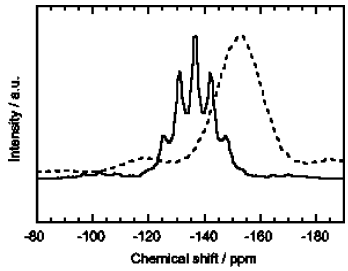

Figure 5. Solid-state ^{31}P NMR spectra of **1**·H_2O (solid line) and **1** (dotted line) at 298 K.

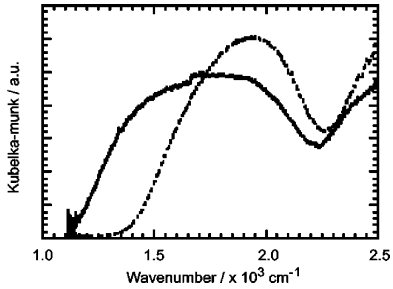

Figure 6. UV−vis reflection spectra of **1**·H_2O (solid line) and **1** (dotted line).

effect of the paramagnetic Cu(II) ions.[12] The spectral change observed in the ^{31}P NMR measurements is explained as follows. In **1**·H_2O, there are free PF_6^- anions in the crystal, which is confirmed by the single-crystal X-ray diffraction measurements and the solid-state ^{31}P NMR spectra. After removal of the H_2O molecules, the PF_6^- anions approach the axial sites of the Cu(II) centers. The UV−vis reflection spectra of **1** (Figure 6) show a broad peak with an absorption maximum of 20.0×10^3 cm^{-1}, assigned to the d−d transition of the Cu(II) ion. Table 2 lists the absorption maxima for [CuX(acac)(tmen)] (X = anion) in the solid state. The stronger the donor ability of the anion, the smaller the value of the absorption maxima. As shown in Table 2, the peak position of **1** is almost the same as for [Cu(acac)-(tmen)]·BPh_4. Therefore, it is expected that the interaction of the PF_6^- anion with the Cu(II) ions is very weak in the solid state. On the other hand, the UV−vis reflection spectrum of **1**·H_2O (Figure 6) has a broad peak with an absorption maximum of 17.1 cm^{-1}, whose value is similar to that of the UV−vis spectra of **1** in H_2O solution (16.9 cm^{-1}, see Supporting Information, Figure S3) but is different from that of the UV−vis reflection spectrum of **1**. These results are consistent with the XRD, TGA, and ^{31}P NMR results.

Similar experiments to those performed on **1** were performed on **2** to compare the binding properties in solution and the solid state. The UV−vis spectrum of **2** in DCE shows a broad peak with an absorption maximum of 18.9 cm^{-1}, whose value is similar to that previously reported (19.0 cm^{-1}, see Table 2 and Supporting Information, Figure S4).[2c] When the dehydrated compound **2** was exposed to H_2O vapor, the rebinding of the H_2O molecules at the Cu(II) axial site was observed. The color of the sample showed a similar change as **1**. In the TGA profile of the exposed compound (Figure 4), the observed weight loss of about 8.8% up to 310 K corresponds to the removal of the H_2O molecules from the compound, which shows that the complex−H_2O ratio was 1:1. Therefore, the exposed compound has the formula [Cu(acac)(tmen)(H_2O)]·BF_4 (**2**·H_2O).

Interestingly, a difference in the stability of the H_2O molecules was observed in **1**·H_2O and **2**·H_2O. From the results of TGA curves of **1**·H_2O and **2**·H_2O (Figure 4), it was revealed that the H_2O molecules of **1**·H_2O are removed in the temperature range 312 to 345 K, while the H_2O molecules of **2**·H_2O start to be eliminated at room temperature, and the H_2O molecules are completely removed at 308 K. Because the absorption maxima of **1** and **2** in H_2O are almost the same (see Supporting Information, Figure S3), there is no large difference in the Cu−O bond lengths in **1**·H_2O and **2**·H_2O. The easy replacement of H_2O molecules by BF_4^- anions in **2**·H_2O was also confirmed by our XRD measurements. The XRD pattern of the sample immediately after the exposure of **2** to H_2O vapor is similar to that of desolvated **2** (Supporting Information, Figure S5), while the color of the sample changed from purple to blue before the XRD measurements. This result implies that the heat originating from the X-ray irradiation induces the rapid removal of the H_2O molecules in **2**·H_2O. The UV−vis reflection spectrum of **2** (Supporting Information, Figure S7) shows a broad peak with an absorption maximum of 18.0×10^3 cm^{-1}. On the other hand, the corresponding spectrum of **2**·H_2O broadens and has an absorption maximum of 17.4×10^3 cm^{-1}, whose value is slightly larger than that of the UV−vis spectra of **2** in H_2O (16.9 cm^{-1}, see Supporting Information, Figure S3). This peak shift was attributed to the partial desorption of the H_2O molecules during the measurement. The time-dependent UV−vis reflection spectra of **1**·H_2O and **2**·H_2O also provide evidence of a gradual desorption of the H_2O molecules (see Supporting Information, Figures S6 and S7). The donor ability of the BF_4^- anion is stronger than that of the PF_6^- anion, which stimulates a rapid axial−ligand exchange in **2**.

Another interesting point is the difference in the thermal properties of **1** and **2**. From the results of the DTA curves (Supporting Information, Figures S1 and S8), the melting points of **1** and **2** were determined to be 423 and 445 K, respectively. In general, the larger the molecular weight, the higher is the melting point. However, these results show the opposite tendency. Because the PF_6^- anion binds to the Cu(II) ion more loosely than the BF_4^- ion does, the PF_6^- anion has a more dynamic nature than the BF_4^- anion in the solid state. Such a characteristic of the PF_6^- anion induces a lower melting point in **1** compared to **2**.

Conclusions

The binding properties of the solvatochromic indicators [Cu(X)(acac)(tmen)] (X = PF_6^- (**1**) and BF_4^- (**2**)) in solution and the solid state have been studied.

First, the donor ability of the PF_6^- anion was determined from the UV−vis spectrum of **1** in DCE. The value of DN_{PF6} is slightly larger than that of DN_{BPh4}, indicating that the PF_6^-

(12) La Mar, G. N.; Horrocks, W. D., Jr.; Holm, R. H. *NMR of Paramagnetic Molecules: Principles and Applications*; Academic Press: New York, 1973.

anion hardly coordinates to the metal center. Therefore, chemists can use the PF_6^- anion as an inert coordination unit as well as BPh_4^-.

Second, the binding properties of **1** in the solid state have been studied. Desolvated **1** forms a weak Cu(II)···PF_6^- interaction. When **1** was exposed to H_2O vapor, an axial ligand exchange occurred to form **1**·H_2O. The adsorption and desorption of the H_2O molecules is reversible with a corresponding color change. Therefore, **1** may be a good solid indicator for Lewis base molecules.

Third, the binding properties of **1** have been compared to those of **2**. Although **2** reversibly binds and releases H_2O molecules as well as **1**, the adsorbed H_2O molecules in **2** are more easily removed from the Cu(II) axial sites than in **1**. Such phenomena can be interpreted as follows. The donor ability of the BF_4^- anion is stronger than that of the PF_6^- anion, which stimulates a rapid release of the H_2O molecules in **2**. Desolvated **1** has a lower melting point compared to **2**, which can be explained by the dynamic nature of the PF_6^- anion loosely binding to the Cu(II) ions.

In this study, we confirmed that Cu(II) coordination complexes have the ability to attract the PF_6^- anion at the axial sites because of the Jahn−Teller effect and electrostatic interactions. Because the Cu(II)−PF_6^- bond is weak, its binding changes flexibly with external stimuli. We are now progressing to create Cu(II) coordination complexes with flexible Cu(II)−PF_6^- parts to develop unprecedented binding properties.

Acknowledgment. This work was supported by a program, Exploratory Research for Advanced Technology (ERATO), Japan Science and Technology (JST). We would like to thank Ms. Ai Tokumitsu and Ms. Miwa Kiuchi (Center for Instrument Analysis, Hokkaido University) for carrying out the elemental analysis. We thank Prof. M. Kato and Dr. Atsushi Kobayashi of Hokkaido University for allowing the use their UV−vis reflection spectral apparatus.

Supporting Information Available: . X-ray crystallographic data for **1**·H_2O in CIF format. TG−DTA curves of **1** and **2**. Photographs of DCE, MeCN, and DMF solutions of **1**. UV−vis spectra of **1** and **2** in H_2O solution. UV−vis spectra of **2** in DCE solution. XRD pattern of **2** and the sample immediately after the exposure of **2** to H_2O vapor. UV−vis reflection spectra of **1** and **2**. Time-dependent UV−vis reflection spectra of **1**·H_2O and**2**·H_2O. This material is available free of charge via the Internet at http://pubs.acs.org.

IC800685Z